

**EFFECT OF THERMOPHORESIS AND HALL EFFECTS ON UNSTEADY MHD CONVECTIVE HEAT AND MASS TRANSFER FLOW OF A VISCOUS ROTATING FLUID PAST A STRETCHING SURFACE WITH THERMAL RADIATION, THERMO-DIFFUSION, RADIATION ABSORPTION IN PRESENCE OF NON-UNIFORM HEAT SOURCE**

**DR. M. SREEVANI**  
Department of Mathematics,  
S.K.U. Engineering College, Anantapuramu – 515003, (A.P.), India.

(Received On: 21-11-18; Revised & Accepted On: 07-01-19)

---

**ABSTRACT**

To the author knowledge no studies have been made to analyze the combined influence of thermo-diffusion and radiation absorption effects on unsteady heat and mass transfer flow of a viscous incompressible electrically conducting fluid over a stretching sheet with thermal radiation, non-uniform heat source/sink and thermophoresis particle deposition. Hence, this problem is addressed in this paper. The conservation of mass, momentum, energy and diffusion equations were transformed into a two-point boundary value problem. In this article, we employ an extensively validation, highly efficient, variational finite-element method to study the effect of unsteadiness on heat and mass transfer flow past a semi-infinite stretching sheet. The problem presented here has many practical applications, such as, technological, manufacturing industries. MHD generators, plasma studies, nuclear reactors, geothermal energy extractions and polymer extrusion. Non-linear stretching velocity, surface temperature and surface concentration are considered in the present paper. The nonlinearity of the basic equations are additional mathematical difficulties associated with it, have led to the use of numerical method.

**Keywords:** Thermophoresis, Stretching Sheet, Thermal Radiation, Sorte Effect, Hall Effect.

---

**1. INTRODUCTION**

In recent years, it is found that thermophoresis is a phenomenon has many practical applications in removing small particles from gas streams, in determining exhaust gas particle trajectories from combustion devices, and in studying the particulate material deposition on turbine blades. It has been found that thermophoresis is the dominant mass transfer mechanism in the modified chemical vapor deposition (MCVD) process as currently used in the fabrication of optical fiber performs. Thermophoretic deposition of radioactive particles is considered to be one of the important factors causing accidents in nuclear reactors. A number of analytical and experimental papers in thermophoretic heat and mass transfer have been communicated. Talbot *et al.* [43] presented a seminal study, considering boundary layer flow with thermophoretic effects, which has become a benchmark for subsequent studies. Several authors, Duwairi and Damseh *et al.* [12], Damseh *et al.* [8], Mahdy and Hady [23], Liu *et al.* [22], Postelnicu [32], Dinesh and Jayaraj [9], Grosan *et al.* [15], Tsai and Huang [44] have investigated the effect of thermophoresis in vertical plate, micro-channel, horizontal plate and parallel plate.

The engineering applications of such flows exist in chemical and food processing industry, centrifugal filtration process, rotating machinery and design of multi-pore distributor in a gas-solid fluidized bed, Pioneering study on the three-dimensional rotating viscous flow induced by a stretching surface was presented by Wang [49]. His problem was governed by an interesting parameter  $\lambda$  that signifies the ratio of the rotation to the stretching rate. He constructed series solutions for small values of parameter  $\lambda$  by regular perturbation approach. He found that velocity distribution (above the sheet) decreases upon increasing this parameter  $\lambda$ . Rajeswari and Nath [33] and Nazar *et al.* [28] extended the Wang's work for unsteady case. Their results indicate a smooth transition from initial unsteady flow to final steady-state flow. Homotopy solutions for rotating flow of non-Newtonian second grade fluid were provided by Hayat *et al.* [18]. They observed that fluid velocity has direct relationship with material parameter of second grade fluid. Zaimi *et al.* [51] examined the rotating flow of viscoelastic fluid bounded by a stretching surface and concluded that boundary layer thickness is an increasing function of visco-elastic fluid parameter. Rashidi *et al.* [35] investigated entropy generation in steady MHD flow due to a rotating porous disk in a nanofluid. Sheikholeslami *et al.* [38] reported

---

**Corresponding Author: Dr. M. Sreevani, Department of Mathematics,  
S.K.U. Engineering College, Anantapuramu – 515003, (A.P.), India.**

numerical results of nanofluid flow and heat transfer in a rotating system with the consideration of magnetic field effects. Mustafa [27] used Cattaneo-Christov heat flux model to investigate the rotating flow of visco-elastic fluid bounded by a stretching surface.

The problem of two dimensional boundary layer flow, heat and mass transfer over a continuous stretching heated surface through porous medium finds numerous and wide range of applications in many engineering and manufacturing disciplines. In industry, polymer sheets and filaments are manufactured by continuous extrusion of the polymer from a die. The thin polymer sheet constitutes of continuously moving surface with a non-uniform velocity through an ambient fluid. The problem of heat and mass transfer flow due to stretching sheet has been implemented on many flow situations. The problem of steady two dimensional viscous incompressible fluid caused by a stretching sheet was first examined by Sikiadis [39]. The thermal behavior of the problem was experimentally verified by Tsou *et al.* [46]. Crane [7] has studied the flow past a stretching plate by taking velocity varying linearly with a distance from a fixed point and this problem is the extension of Sikiadis[39]. Gupta *et al.* [17] have studied heat and mass transfer characteristics of stretching sheet with suction or blowing. Grubka and Bobba [16] studied the heat transfer characteristics over a continuous stretching surface with variable temperature. Ali [2] has investigated flow a heat transfer characteristics on a continuous stretching surface using power-law velocity and temperature distributions. Vajravelu [47] has analyzed the study of flow and heat transfer in saturated porous medium over an impermeable stretching sheet. Two cases have been discussed in this problem, (i) the sheet with prescribed sheet temperature (PST-case) and (ii) the sheet with prescribed wall flux (PHF-case).

In all the previous investigations, the effects thermal radiation and magnetic field on the flow and heat transfer have not been studied. It is well known the radiative heat transfer flow is very important in manufacturing industries for the design of reliable equipment's, nuclear plants, gas turbines and various propulsion devices for aircraft, missiles, satellites and space vehicles. Also, the effects of thermal radiation on forces and free convection flow are important in the content of space technology and process involving high temperature. Recent developments in hypersonic flights, missile reentry rocket combustion chambers, gas cooled nuclear reactors and power plants for inter planetary flight, have focused attention of researchers on thermal radiation as a mode of energy transfer, and emphasize the need for inclusion of radiative transfer in these process. Magneto nanofluids have specific applications in biomedicine, optical modulators, magnetic cell separation, magneto-optical wavelength filters, silk float separation, nonlinear optical materials, hyperthermia, optical switches, drug delivery, optical gratings etc. A magnetic nanofluid has both the liquid and magnetic properties. The used magnetic field influences the suspended particles and reorganizes their concentration in the fluid regime which powerfully influences the heat transfer analysis of the flow. Magneto nanofluids are useful to guide the particles up the blood stream to a tumor with magnets. This is due to the fact that the magnetic nanoparticles are regarded more adhesive to tumor cells than non-malignant cells. Such particles absorb more power than micro particles in alternating current magnetic fields tolerable in humans i.e. for cancer therapy, Plumb *et al.* [31] was the first to examine the effect of horizontal cross flow and radiation on natural convection from vertical heated surface in a saturated porous media. Recently, Pal D *et al.* [29] has discussed radiation effect on hydro magnetic Darcy Forchheimer mixed convection flow over stretching sheet. Mansour and El-Shaer [25] analyzed the effects of thermal radiation on magneto hydrodynamic natural convection flows in a fluid saturated porous media. Pal [30] studied heat and mass transfer in stagnation-point flow toward a stretching sheet in the presence of buoyancy force and thermal radiation. Vajravelu and Rollins [48] studied heat transfer in electrically conducting fluid over a stretching sheet by taking into account of magnetic field only. Molla *et al.* [26] studied the effect of thermal radiation on a steady two-dimensional natural convection laminar flow of viscous incompressible optically thick fluid along a vertical flat plate with stream wise sinusoidal surface temperature. Abo-Eldahab and El-Gendy [1] investigated the problem of free convection heat transfer characteristics in an electrically conducting fluid near an isothermal sheet to study the combined effect of buoyancy and radiation in the presence of uniform transverse magnetic field.

In the case of binary mixtures, the species gradients can be established by the applied boundary conditions such as species rejection associated with alloys costing, or can be induced by transport mechanism such as Soret (thermo) diffusion. In the case of Soret diffusion, species gradients are established in an otherwise uniform concentration mixture in accordance with Onsager reciprocal relationship. Thermal-diffusion known as the Soret effect takes place and as a result a mass fraction distribution is established in the liquid layer. The sense of migration of the molecular species is determined by the sign of Soret coefficient. Soret and Dufour effects are very significant in both Newtonian and non-Newtonian fluids when density differences exist in flow regime. The thermo-diffusion (Soret) effect is corresponds to species differentiation developing in an initial homogeneous mixture submitted to a thermal gradient and the diffusion thermo (Dufour) effect corresponds to the heat flux produced by a concentration gradient. Dulal Pal *et al.* [10] has studied MHD non-Darcian mixed convection heat and mass transfer over a non-linear stretching sheet with Soret and Dufour effects and chemical reaction. MHD mixed convection flow with Soret and Dufour effects past a vertical plate embedded in porous medium was studied by Makinde [24], Reddy *et al.* [36] has presented finite element solution to the heat and mass transfer flow past a cylindrical annulus with Soret and Dufour effects. Chamkha *et al.* [6] has studied the influence of Soret and Dufour effects on unsteady heat and mass transfer flow over a rotating vertical cone and they suggested has temperature and concentration fields are more influenced with the values of Soret and Dufour parameter.

In all the above studies the physical situation is related to the process of uniform stretching sheet. For the development of more physically realistic characterization of the flow configuration it is very useful to introduce unsteadiness into the flow, heat and mass transfer problems. The working fluid heat generation or absorption effects are very crucial in monitoring the heat transfer in the regions, heat removal from nuclear fuel debris, underground disposal of radiative waste material, storage of food stuffs, exothermic chemical reactions and dissociating fluids in packed-bed reactors. This heat source can occur in the form of a coil or battery. Very few studies have been found in literature on unsteady boundary flows over a stretching sheet by taking heat generation/absorption into the account. Wang CY [50] was first studied the unsteady boundary layer flow of a liquid film over a stretching surface. Later, Elbashaeshy and Bazid [13] has presented the heat transfer over an unsteady stretching surface. Tsai *et al* [45] has discussed flow and heat transfer characteristics over an unsteady stretching surface by taking heat source into the account. Ishak *et al.* [19] analyzed the effect of prescribed wall temperature on heat transfer flow over an unsteady stretching permeable surface. Ishak [20] has presented unsteady MHD flow and heat transfer behavior over a stretching plate. Recently, Dulal Pal [11] has described the analysis of flow and heat transfer over an unsteady stretching surface with non-uniform heat source/sink and thermal radiation. Dulal Pal *et al.* [11] have presented MHD non-Darcian mixed convection heat and mass transfer over a non-linear stretching sheet with Soret Dufour effects, heat source/sink and chemical reaction. Sreenivasa Reddy [41] has discussed Soret and Dufour effect on convective heat and mass transfer flow of micro polar fluid in the presence of thermophoresis. Sreeniva Reddy [42] has discussed the effect of thermophoresis on unsteady mixed convective heat and mass transfer flow past stretching sheet with thermal radiation, Soret and Dufour effect in the presence of non uniform heat source. Aliveni *et al.* [3] have discussed soret and dufour effects on convective heat and mass transfer flow of a viscous fluid in the presence of thermophoresis deposition particle. Sivagopal *et al.* [40] have discussed Soret and Dufour effects on MHD heat and mass transfer flow of a micropolar fluid over stretching sheet through porous medium with thermophoresis.

**2. FORMULATION OF THE PROBLEM:**

We analyse the transient convective heat and mass transfer flow of an electrically conducting fluid past a stretching sheet with the plane at  $y=0$  and the flow is confined to the region  $y>0$ . A schematic representation of the physical model is exhibited in fig.1. We choose the frame of reference  $O(x,y,z)$  such that the  $x$ -axis is along the direction of motion of the surface, the  $y$ -axis is normal to the surface and  $z$ -axis transverse to the  $(x-y)$  plane. An uniform magnetic field of strength  $H_0$  is applied in the positive  $y$ -direction. The surface of the sheet is assumed to have a variable temperature and concentration  $T_w(x)$ , and  $C_w(x)$  respectively, while the ambient fluid has a uniform temperature and concentration  $T_\infty$  and  $C_\infty$ , where  $T_w(x) > T_\infty$ ,

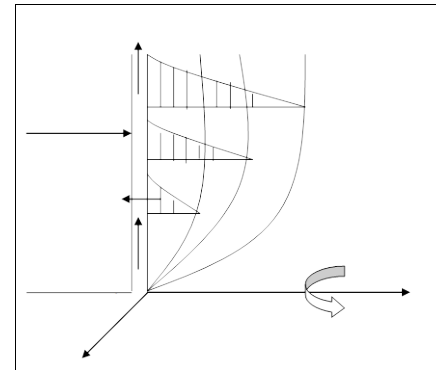


Fig.1 : Flow configuration and coordinate system

$C_w(x) > C_\infty$  corresponds to a heated plate and  $T_w(x) < T_\infty$ ,  $C_w(x) < C_\infty$  corresponds to a cooling plate. The flow is assumed to be confined in the region  $y>0$ . We consider a non-uniform internal heat generation/absorption source in the flow to get the temperature and concentration differences between the surface and ambient fluid. We that the velocity is proportional to its distance from the slit. We consider Hall effects into consideration and assume the electron pressure gradient, the ion-slip and the thermo-electric effects are negligible. Using boundary layer approximation, Boussinesq's approximation the basic equations governing the flow, heat and mass transfer under Rosseland approximation are

$$\frac{\partial u}{\partial x} + \frac{\partial v}{\partial y} = 0 \tag{2.1}$$

$$\frac{\partial u}{\partial t} + u \frac{\partial u}{\partial x} + v \frac{\partial u}{\partial z} = \nu \frac{\partial^2 u}{\partial y^2} + \beta g(T - T_\infty) + \beta^* g(C - C_\infty) - \frac{\sigma B_0^2}{\rho(1 + m^2)}(u + mw) \tag{2.2}$$

$$\frac{\partial w}{\partial t} + u \frac{\partial w}{\partial z} + v \frac{\partial w}{\partial z} = \nu \frac{\partial^2 w}{\partial y^2} + \frac{\sigma B_0^2}{\rho(1 + m^2)}(mu - w) \tag{2.3}$$

$$\rho C_p \left( \frac{\partial T}{\partial t} + u \frac{\partial T}{\partial x} + v \frac{\partial T}{\partial y} \right) = k_f \frac{\partial^2 T}{\partial y^2} + \frac{k_f U_w(x,t)}{xv} (A_1(T_w - T_\infty) f' + (T - T_\infty) B_1) + \tag{2.4}$$

$$\mu \left[ \left( \frac{\partial u}{\partial y} \right)^2 + \left( \frac{\partial w}{\partial y} \right)^2 \right] + \frac{16\sigma^* T_\infty^3}{3\beta_R} \frac{\partial^2 T}{\partial y^2} \tag{2.5}$$

$$\left( \frac{\partial C}{\partial t} + u \frac{\partial C}{\partial x} + v \frac{\partial C}{\partial y} \right) = D_B \frac{\partial^2 C}{\partial y^2} + \frac{D_m K_T}{T_m} \frac{\partial^2 T}{\partial y^2} - \frac{\partial(V_T C)}{\partial y}$$

The relevant boundary conditions are

$$u = U_w(x,t) + L \frac{\partial u}{\partial y}, v = V_w, T = T_w, C = C_w \quad \text{at } y = 0 \tag{2.6}$$

$$u \rightarrow 0, T \rightarrow T_\infty, C \rightarrow C_\infty \quad \text{as } y \rightarrow \infty$$

Where T is the temperature, C is the concentration inside the boundary layer, u, v and w are the velocity components along x, y and z-directions respectively, Cp is the specific heat at constant pressure, Cs is the concentration susceptibility, ρ is the density of the fluid, kf is the thermal conductivity, μ is the fluid viscosity, ν is the kinematic viscosity, Tw(x,t) is the stretching surface temperature, Cw(x,t) is the concentration of the stretching surface, T∞ is the temperature far away from the stretching surface with Tw > T∞, C∞ is the concentration far away from the stretching surface with Cw > C∞. The term Vw = -√(νUw/2x) f(0) represents the mass transfer at the surface with Vw > 0 for suction and Vw < 0 for injection.

The coefficient q''' is the rate of internal heat generation (>0) or absorption (<0). The internal heat generation /absorption q''' is modeled as

$$q''' = \frac{k_f U_w(x,t)}{x\nu} (A_1(T_w - T_\infty) f' + (T - T_\infty) B_1) \tag{2.7}$$

where A1 and B1 are coefficients of space dependent and temperature dependent internal heat generation or absorption respectively. It is noted that the case A1 > 0 and B1 > 0, corresponds to internal heat generation and that A1 < 0 and B1 < 0, the case corresponds to internal heat absorption case.

Due to stretching of the sheet the flow is caused and it moves with the surface velocity, temperature and concentration of the form

$$U_w(x,t) = \frac{ax}{1-ct}, T_w(x,t) = T_\infty + \frac{ax}{1-ct}, C_w(x,t) = C_\infty + \frac{ax}{1-ct} \tag{2.8}$$

where a is stretching rate and c are positive with ct < 1, c ≥ 0. It is noticed that the stretching rate ax/(1-ct) increases with time t since a > 0.

The stream function ψ(x,t) is defined as:

$$u = \frac{\partial \psi}{\partial y} = \frac{ax}{(1-ct)} f'(\eta), v = -\frac{\partial \psi}{\partial x} = \frac{av}{(1-ct)} f(\eta) \tag{2.9}$$

On introducing the similarity variables (Dulal Pal [10]):

$$\eta = \sqrt{\frac{a}{(1-ct)}} y,$$

$$u = \frac{ax}{1-ct} f'(\eta), v = -\sqrt{\frac{va}{1-ct}} f(\eta), w = \frac{ax}{1-ct} g(\eta), \tag{2.10}$$

$$\theta(\eta) = \frac{T - T_\infty}{T_w - T_\infty}, \phi = \frac{C - C_\infty}{C_w - C_\infty}$$

$$B^2 = B_o^2 (1-ct)^{-1}$$

where T is the temperature and C is the concentration in the fluid. kf is the thermal conductivity, Cp is the specific heat at constant pressure, β is the coefficient of thermal expansion, β\* is the volumetric expansion with concentration, Q1<sup>1</sup> is the radiation absorption coefficient, qr is the radiative heat flux, kc is the chemical reaction coefficient, DB is the molecular viscosity, Dm, KT, Tm mean fluid temperature, k is the porous permeability parameter.

The effect of thermophoresis is usually prescribed by means of average velocity acquired by small particles to the gas velocity when exposed to a temperature gradient. In boundary layer flow, the temperature gradient in the y-direction is very much larger than in the x-direction and therefore only the thermophoresis velocity in y-direction is considered. As a consequence, the thermophoresis velocity VT, which appears in equation (2.5) is expressed as

$$V_T = -\frac{k_1 \nu}{T_r} \frac{\partial T}{\partial y} \tag{2.11}$$

In which  $k_1$  is the thermophoresis coefficient and  $T_r$  is the reference temperature. A thermophoresis parameter  $\tau$  is given by the relation

$$\tau = -\frac{k_1(T_w - T_\infty)}{T_r} \tag{2.12}$$

Where the typical values of  $\tau$  are 0.01, 0.1 and 1.0 corresponding to approximate values of  $k_1(T_w - T_\infty)$  equal to 3,30,300K for a reference temperature of  $T = 300K$

Using Equations (2.10) & (2.12) into equations (2.2)-(2.5) we get

$$f''' + ff'' - (f')^2 - S(f' - 0.5\eta f'') - \frac{M^2}{1+m^2}(f' + mg) + G(\theta + N\phi) = 0 \tag{2.13}$$

$$g'' + fg' - f'g - S(g' + 0.5g'') + \frac{M^2}{1+m^2}(mf' - g) = 0 \tag{2.14}$$

$$(1 + \frac{4Rd}{3})\theta'' + Pr(f\theta' - f'\theta) - PrS(\theta + 0.5\eta\theta') + (A_1f' + B_1\theta) + PrEc((f'')^2 + (g'')^2) + \frac{EcM^2}{1+m^2}((f')^2 + g^2) = 0 \tag{2.15}$$

$$\phi'' + -Sc(2f'\phi - f\phi') - ScS(\phi + 0.5\eta\phi') + ScSr\theta'' - \tau(\theta'\phi' + \theta''\phi) = 0 \tag{2.16}$$

Where  $S=c/a$  is the unsteadiness parameter.  $M = \frac{\sigma B_0^2}{\rho a}$  is the magnetic parameter,

$D^{-1} = \frac{\nu}{ak}$  is the inverse Darcy parameter,  $G = \frac{\beta g(T_w - T_\infty)}{U_w \nu_w^2}$  is the thermal buoyancy parameter,

$N = \frac{\beta^*(C_w - C_\infty)}{\beta(T_w - T_\infty)}$  is the buoyancy ratio,  $Pr = \frac{\mu C_p}{k_f}$  is the Prandtl number,  $Ec = \frac{U_w^2}{C_p(T_w - T_\infty)}$  is the Eckert

number,  $Sc = \frac{\nu}{D_B}$  is the Schmidt number,  $m = \omega_e \tau_e$  is the Hall parameter and  $Sr = \frac{D_m K_T (T_w - T_\infty)}{\nu T_m (C_w - C_\infty)}$  is the Soret parameter.

It is pertinent to mention that  $\gamma > 0$  corresponds to a degenerating chemical reaction while  $\gamma < 0$  indicates a generation chemical reaction.

The transformed boundary conditions (2.6) & (2.10) reduce to

$$\begin{aligned} f'(0) &= 1 + Af''(0), f(0) = fw, \theta(0) = 1, \phi(0) = 1 \\ f'(\infty) &\rightarrow 0, g(\infty) \rightarrow 0, \theta(\infty) \rightarrow 0, \phi(\infty) \rightarrow 0 \end{aligned} \tag{2.17}$$

Where  $fw = \frac{\nu_w}{\sqrt{av}}$  is the mass transfer coefficient such that  $fw > 0$  represents suction and  $fw < 0$  represents injection at the surface.

### 3. METHOD OF SOLUTION

The finite element method is a powerful technique for solving ordinary or partial differential equations. The steps involved in the finite element analysis are as follows:

- Discretization of the domain into elements
- Derivation of element equations
- Assembly of element equations
- Imposition of boundary conditions
- Solution of assembled equations

The whole flow domain divided into 1000 quadratic elements of equal size. Each element is three-noded and therefore the whole domain contains 2001 nodes. We obtain a system of equations contains 8004 equations. The obtained system is non-linear, therefore an iterative scheme is utilized in the solution. After imposing the boundary conditions the remaining system contains 7997 equations, which is solved by the Gauss elimination method while maintaining an accuracy of  $10^{-5}$ .

#### 4. SKIN FRICTION, NUSSLETT NUMBER AND SHERWOOD NUMBER

The physical quantities of engineering interest in this problem are the skin friction coefficient  $C_f$ , the Local Nusselt number ( $Nu_x$ ), the Local Sherwood number ( $Sh_x$ ) which are expressed as

$$\frac{1}{2} C_f \sqrt{R_{ex}} = f''(0), \quad \frac{1}{2} C_{fz} \sqrt{R_{ez}} = g'(0), \quad Nu_x / \sqrt{R_{ex}} = 1 / \theta(0), \quad Sh_x / \sqrt{R_{ex}} = 1 / \phi(0)$$

where  $\mu = \frac{k}{\rho C_p}$  is the dynamic viscosity of the fluid and  $R_{ex}$  is the Reynolds number.

For the computational purpose and without loss of generality  $\infty$  has been fixed as 8. The whole domain is divided into 11 line elements of equal width, each element being three noded.

#### 5. RESULTS AND DISCUSSION

Comprehensive numerical computations are conducted for different values of the parameters that describe the flow characteristics and the results are illustrated graphically and in tabular form. Selected graphical profiles are presented in figs. 2-18. The comparison of skin friction coefficient  $f''(0)$  for values of  $(Pr)$  with (33) is made and the results are shown in Table 2 in the absence of other parameters.

Figs. 2a-2d represent the variation of velocity, temperature and concentration with Hall parameter ( $m$ ). It can be seen from the velocity profiles that the primary velocity ( $f'$ ) reduces with higher values of  $m$ . While the secondary velocity ( $g$ ) reduces in the region  $(0, 2.0)$  and in the region far away from the sheet the secondary velocity enhances with  $m > 0.5$  and reduces with smaller values of  $m$ . An increase in  $m$  enhances the temperature and reduces the mass concentration. This is attributed to the fact that the thickness of the thermal boundary layer increases while the solutal boundary layer thickness decreases with increase in  $m$ .

Fig. 3a-3d demonstrate the influence of Eckert number on velocity, temperature and concentration. It is pointed that the presence of Eckert number increases the temperature. This is because of the fact that thermal energy is reserved in the fluid on account of friction heating. Hence, the temperature distribution rises in the entire boundary layer. The primary and secondary velocity components rise with increasing values of  $Ec$  owing to the energy release which increases the momentum boundary layer. However, the mass concentration is enhanced marginally with increase in  $Ec$ .

The variation of Soret parameter ( $Sr$ ) on velocities, temperature and concentration are plotted in figs. 4a-4d. It is seen from the profiles that the primary and secondary velocities increase with increasing values of the Soret parameter. Higher the thermo-diffusion effects larger the temperature and mass concentration (figs. 4c & 4d). This may be attributed to the fact the thickness of the thermal and solutal boundary layers increase with increasing  $Sr$ .

The influence of unsteadiness parameter ( $S$ ) on the velocity components, temperature and concentration profiles is shown in figs. 5a-5d. It can be seen that the velocity components, temperature decelerates with increase in the values of unsteadiness parameter ( $S$ ). This is because of the fact that, the motion is generated by the stretching of the sheet and the stretching sheet velocity and temperature is greater than the free stream velocity and temperature, so, the thermal boundary layer thickness decreases with increase in the values of  $S$  as shown in fig. 5c. The concentration profiles also decrease in the flow region and is shown in fig. 5d. It is also observed that the temperature profiles decrease smoothly in the absence of unsteadiness parameter ( $S=0$ ) whereas temperature profiles continuously decrease with the increasing values of unsteadiness parameter. This shows that the rate of cooling is much faster for the higher values of unsteadiness parameter and it takes longer time for cooling in the steady flows.

Figs. 6a-6d show the variation of velocity, temperature and concentration with space dependent heat source parameter  $A_1$ . The presence of the heat source generates energy in the thermal boundary layer and as a consequence the temperature rises. In case heat absorption ( $A_1 < 0$ ) the temperature falls with decreasing values of  $A_1 < 0$  owing to the absorption of energy in the thermal boundary layer. The influence of heat generation is very meagre on the primary velocity when compared to the secondary velocity. In either case both velocities increase with increasing values of heat generating parameter. The effect of heat generation is to enhance the mass concentration marginally.

Figs.7a-7d exhibit the influence of temperature dependent heat source/Sink parameter B1 on velocity, temperature and concentration. As in the case of space dependent heat source, the temperature increases due to the release of thermal energy for  $B1 > 0$  while the temperature drops for decreasing values of  $B1 < 0$  owing to the absorption of energy. The primary and secondary velocities increase for increasing values of heat source parameter ( $B1 > 0$ ) whereas for  $B1 < 0$ , the velocities reduce for decreasing values of  $B1$ . The effect of  $B1$  on mass concentration is similar to that of  $A1$ .

The effect of thermophoresis parameter ( $\tau$ ) on velocity components, temperature and concentration profiles is exhibited in figs.8a-8d. It can be seen from figs.8a&8b that the velocity components depreciate with increase in  $\tau$ . This is due to the fact that an increase in  $\tau$  decreases the thickness of the momentum boundary layer. From fig.8c we find that the temperature profiles experience a deceleration with increase in  $\tau$ . This is because of the fact that the particles near the hot surface create a thermophoretic force. Fig.8d exhibits the impact of  $\tau$  on concentration profiles, it is noticed that the concentration profiles decreases with increase in thermophoretic parameter ( $\tau$ ). This is because of the fact that the fluid moves from hot surface to the cold surface, then the values of thermophoretic parameter have been taken positive. From these two figures we conclude that the imposition of thermophoretic particles deposition into the flow decreases the thickness of thermal and solutal boundary layers.

Figs.9a-9d demonstrate the influence of slip parameter (A) on the velocity, temperature and concentration. It can be seen from the profiles that an increase in the slip parameter (A) reduces the primary and secondary velocities. The temperature rises and the mass concentration drops with increasing values of A.

The variation of thermal radiation parameter ( $R_d$ ) on the velocity, temperature and concentration is depicted in figs.10a-10d. It is observed that there is a significant rise in the primary and secondary velocities in the presence of thermal radiation throughout the boundary layer. The radiation parameter is found to increase the hydrodynamic boundary layer along the x and y-directions. The presence of thermal radiation is very significant on the variation of temperature. It is seen that the temperature increases rapidly in the presence of thermal radiation parameter throughout the thermal boundary layer. This may be attributed to the fact that as the Rosseland radiative absorption parameter  $R^*$  diminishes the corresponding heat flux diverges and thus rising the rate of radiative heat transfer to the fluid causing a rise in the temperature of the fluid. Also an increase in  $R_d$  enhances the concentration profiles.

The skin friction components ( $\tau_x$ ), ( $\tau_y$ ), Nusselt number (Nu) and Sherwood number (Sh) for different  $m$ ,  $S_r$ ,  $Ec$ ,  $\tau$ ,  $A$ ,  $S$ ,  $A1$  and  $B1$ . An increase in Hall parameter ( $m$ ) reduces the skin friction component  $\tau_x$ ,  $Sh$  and enhances  $\tau_y$ , Nusselt number on the wall. When the molecular buoyancy force dominates over the thermal buoyancy force the skin friction component  $\tau_x$  and  $Sh$  reduces while  $\tau_y$  and  $Nu$  increases when the buoyancy forces are in the same direction and for the forces acting in opposite directions,  $\tau_x$ ,  $Sh$  increase, while  $\tau_y$ ,  $Nu$  decrease on the wall. An increase in space dependent heat source parameter smaller  $\tau_x$ ,  $Nu$ ,  $Sh$  and larger  $\tau_y$  on the wall. Decreasing values of  $A < 0$ , reduces  $\tau_x$ , Nusselt and Sherwood numbers and enhances  $\tau_y$  on the wall. An increase in  $B1 > 0$  reduces  $\tau_x$ ,  $Nu$  and  $Sh$  while  $\tau_y$  enhances on the wall. For decreasing values of  $B1 < 0$ , we notice an enhancement in  $\tau_x$ ,  $\tau_y$ ,  $Nu$  and  $Sh$  on the wall = 0. Higher the thermophoretic parameter ( $\tau$ ) larger  $\tau_x$ ,  $Nu$  and  $Sh$  and smaller  $\tau_y$  on the wall. An increase in the slip parameter (A) reduces the skin friction components and Nusselt number and enhances the Sherwood number on the wall. The skin friction component  $\tau_x$ , rate of heat and mass transfer on the wall experience an enhancement with increasing values of unsteadiness parameter  $S$  while  $\tau_y$  reduces with  $S$ .

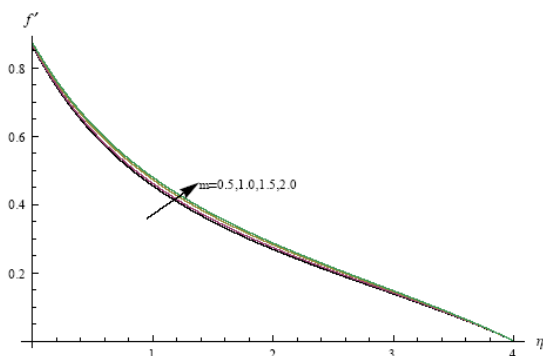


Fig.2a Variation of  $f'(\eta)$  with  $m$   
 $S_r=0.5, A1=0.1, B1=0.1, S=0.2, A=0.2, \tau=0.1$

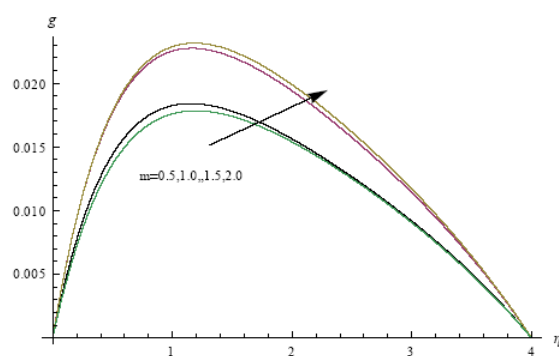


Fig.2b Variation of  $g(\eta)$  with  $m$   
 $S_r=0.5, A1=0.1, B1=0.1, S=0.2, A=0.2, \tau=0.1$

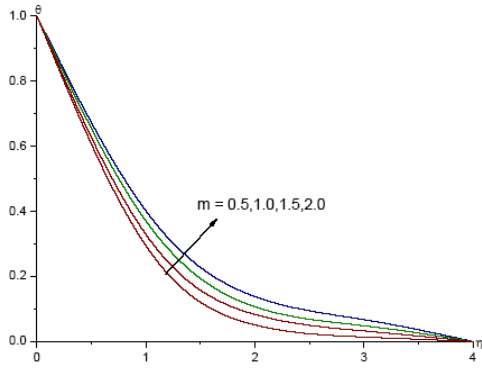


Fig.2c Variation of  $\theta(\eta)$  with  $m$   
 $Sr=0.5, A1=0.1, B1=0.1, S=0.2, A=0.2, \tau=0.1$

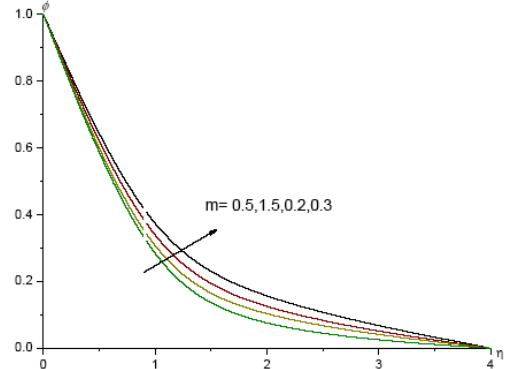


Fig.2d Variation of  $\phi(\eta)$  with  $m$   
 $Sr=0.5, A1=0.1, B1=0.1, S=0.2, A=0.2, \tau=0.1$

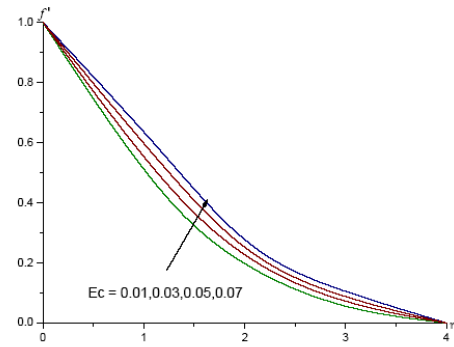


Fig.3a Variation of  $f'(\eta)$  with  $Ec$   
 $Sr=0.5, m=0.5, A1=0.1, B1=0.1, S=0.2, A=0.2, \tau=0.1$

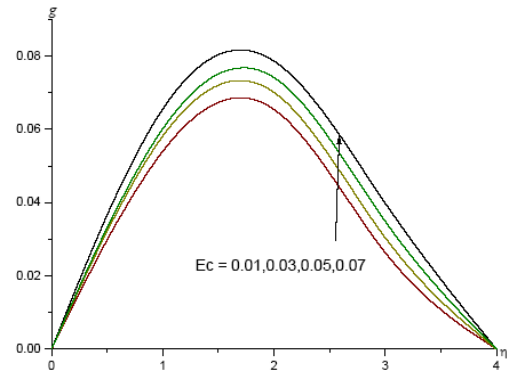


Fig.3b Variation of  $g(\eta)$  with  $Ec$   
 $Sr=0.5, m=0.5, A1=0.1, B1=0.1, S=0.2, A=0.2, \tau=0.1$

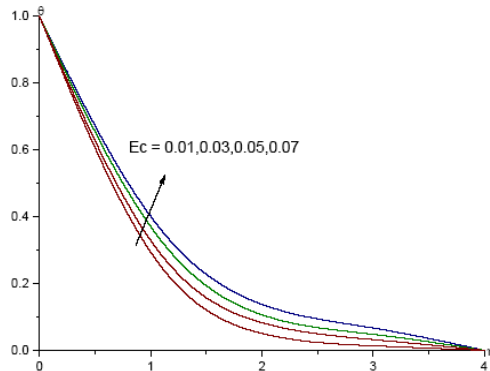


Fig.3c Variation of  $\theta(\eta)$  with  $Ec$   
 $Sr=0.5, m=0.5, A1=0.1, B1=0.1, S=0.2, A=0.2, \tau=0.1$

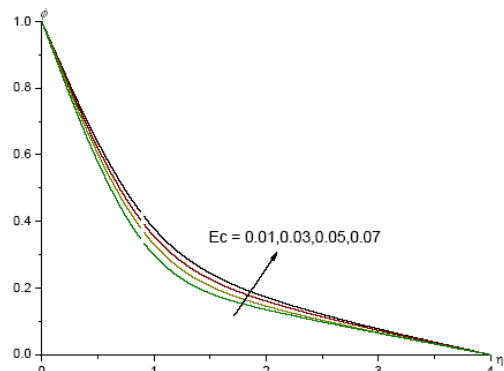


Fig.3d Variation of  $\phi(\eta)$  with  $Ec$   
 $Sr=0.5, m=0.5, A1=0.1, B1=0.1, S=0.2, A=0.2, \tau=0.1$

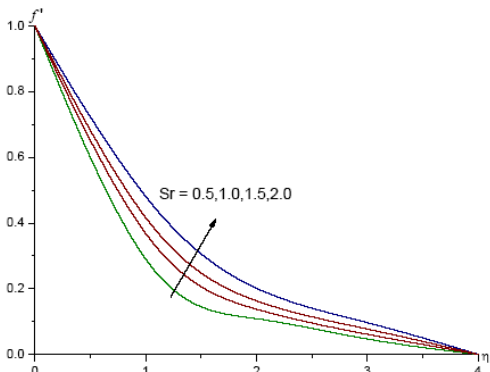


Fig.4a Variation of  $f'(\eta)$  with  $Sr$   
 $Ec=0.01, m=0.5, A1=0.1, B1=0.1, S=0.2, A=0.2, \tau=0.1$

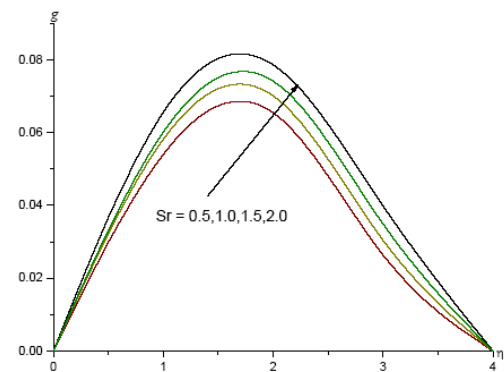


Fig.4b Variation of  $g(\eta)$  with  $Sr$   
 $Ec=0.01, m=0.5, A1=0.1, B1=0.1, S=0.2, A=0.2, \tau=0.1$



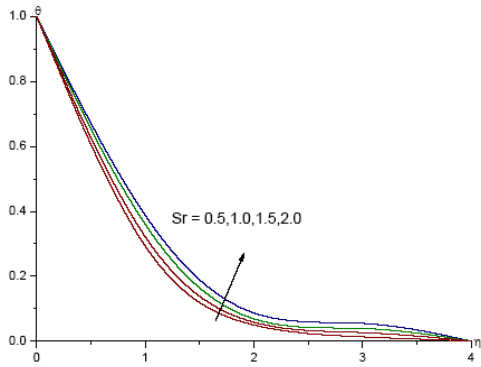


Fig.4c Variation of  $\theta(\eta)$  with Sr  
 $Ec=0.01, m=0.5, A1=0.1, B1=0.1, S=0.2, A=0.2, \tau=0.1$

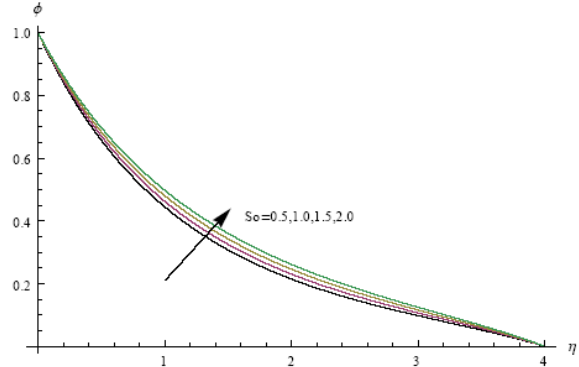


Fig.4d Variation of  $\phi(\eta)$  with Sr  
 $Ec=0.01, m=0.5, A1=0.1, B1=0.1, S=0.2, A=0.2, \tau=0.1$

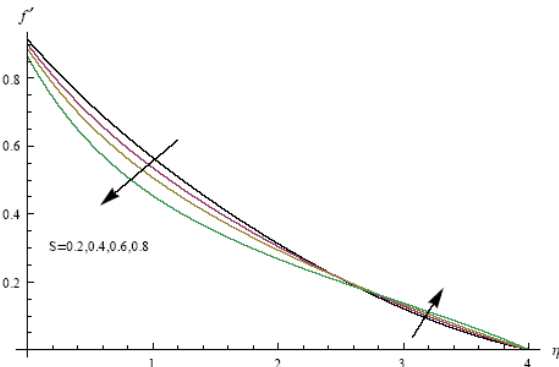


Fig.5a Variation of  $f'(\eta)$  with S  
 $Sr=0.5, Ec=0.01, m=0.5, A1=0.1, B1=0.1, A=0.2, \tau=0.1$

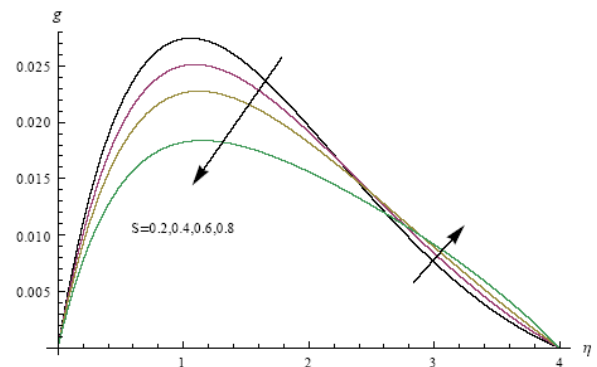


Fig.5b Variation of  $g(\eta)$  with S  
 $Sr=0.5, Ec=0.01, m=0.5, A1=0.1, B1=0.1, A=0.2, \tau=0.1$

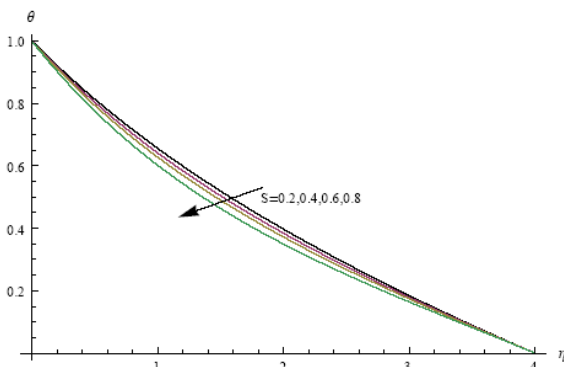


Fig.5c Variation of  $\theta(\eta)$  with S  
 $Sr=0.5, Ec=0.01, m=0.5, A1=0.1, B1=0.1, A=0.2, \tau=0.1$

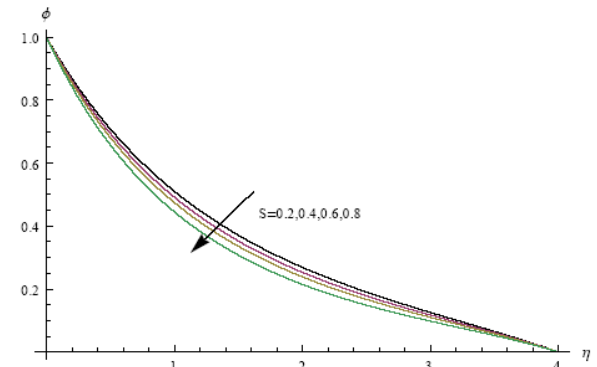


Fig.5d Variation of  $\phi(\eta)$  with S  
 $Sr=0.5, Ec=0.01, m=0.5, A1=0.1, B1=0.1, A=0.2, \tau=0.1$

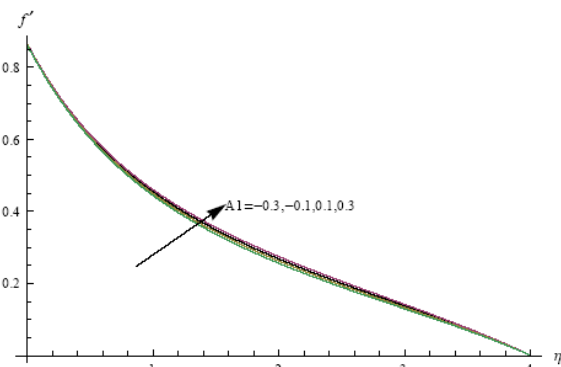


Fig.6a Variation of  $f'(\eta)$  with A1  
 $Sr=0.5, Ec=0.01, m=0.5, S=0.2, B1=0.1, A=0.2, \tau=0.1$

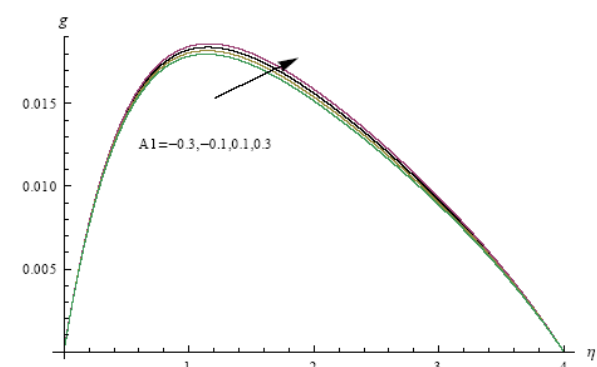


Fig.6b Variation of  $g(\eta)$  with A1  
 $Sr=0.5, Ec=0.01, m=0.5, S=0.2, B1=0.1, A=0.2, \tau=0.1$

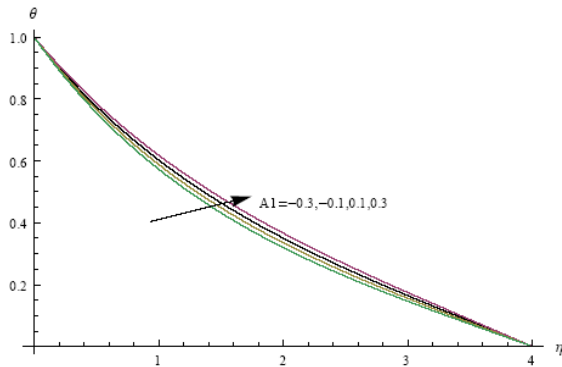


Fig.6c Variation of  $\theta(\eta)$  with  $A1$   
 $Sr=0.5, Ec=0.01, m=0.5, S=0.2, B1=0.1, A=0.2, \tau=0.1$

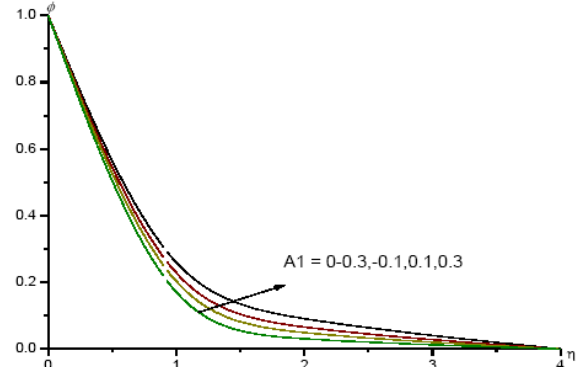


Fig.6d Variation of  $\phi(\eta)$  with  $A1$   
 $Sr=0.5, Ec=0.01, m=0.5, S=0.2, B1=0.1, A=0.2, \tau=0.1$

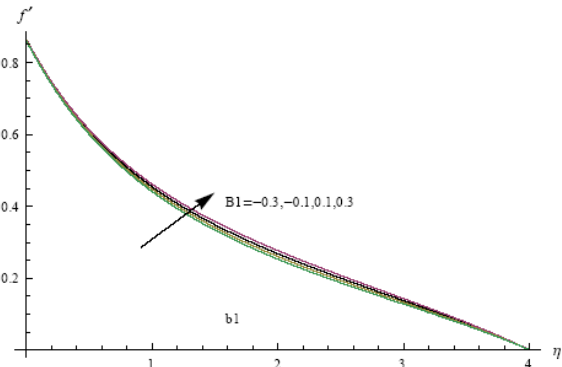


Fig.7a Variation of  $f'(\eta)$  with  $B1$   
 $Sr=0.5, Ec=0.01, m=0.5, S=0.2, A1=0.1, A=0.2, \tau=0.1$

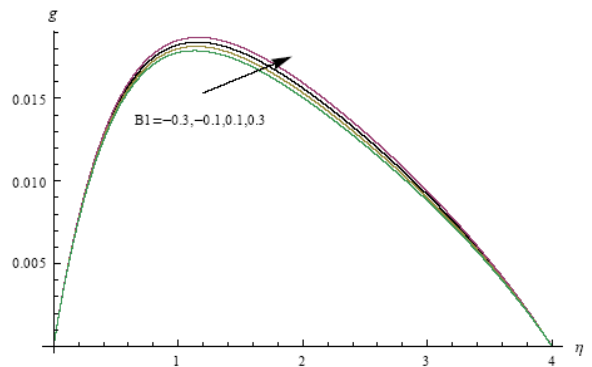


Fig.7b Variation of  $g(\eta)$  with  $B1$   
 $Sr=0.5, Ec=0.01, m=0.5, S=0.2, A1=0.1, A=0.2, \tau=0.1$

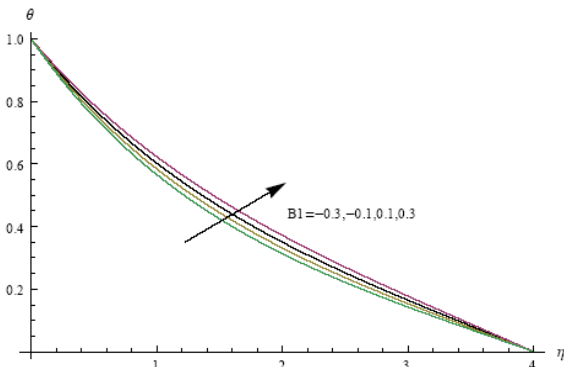


Fig.7c Variation of  $\theta(\eta)$  with  $B1$   
 $Sr=0.5, Ec=0.01, m=0.5, S=0.2, A1=0.1, A=0.2, \tau=0.1$

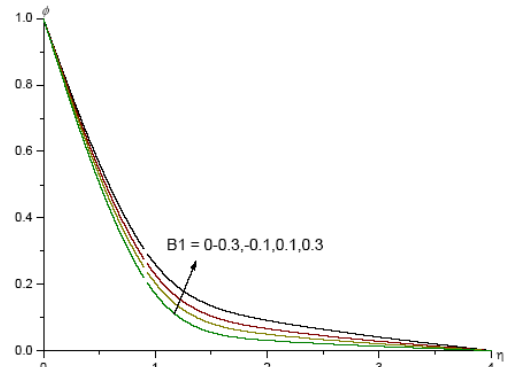


Fig.7d Variation of  $\phi(\eta)$  with  $B1$   
 $Sr=0.5, Ec=0.01, m=0.5, S=0.2, A1=0.1, A=0.2, \tau=0.1$

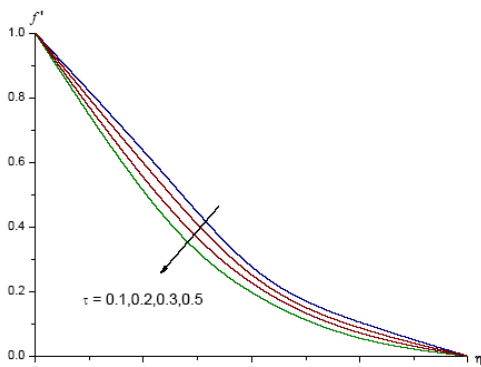


Fig.8a Variation of  $f'(\eta)$  with  $\tau$   
 $Sr=0.5, Ec=0.01, m=0.5, S=0.2, A1=0.1, A=0.2, B1=0.1$

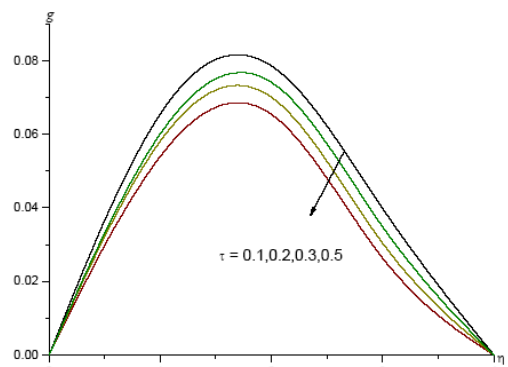


Fig.8b Variation of  $g(\eta)$  with  $\tau$   
 $Sr=0.5, Ec=0.01, m=0.5, S=0.2, A1=0.1, A=0.2, B1=0.1$

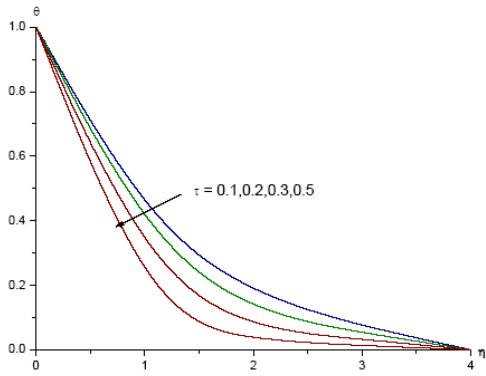


Fig.8c Variation of  $\theta(\eta)$  with  $\tau$   
 $Sr=0.5, Ec=0.01, m=0.5, S=0.2, A1=0.1, A=0.2, B1=0.1$

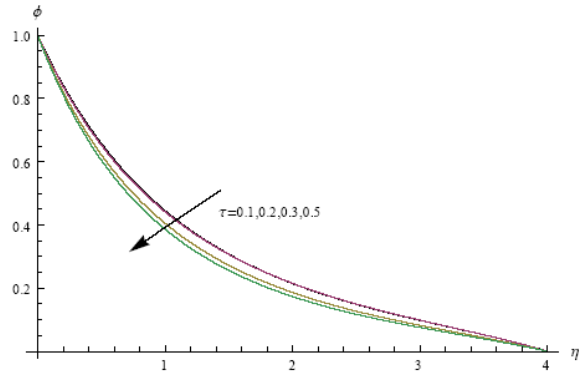


Fig.8d Variation of  $\phi(\eta)$  with  $\tau$   
 $Sr=0.5, Ec=0.01, m=0.5, S=0.2, A1=0.1, A=0.2, B1=0.1$

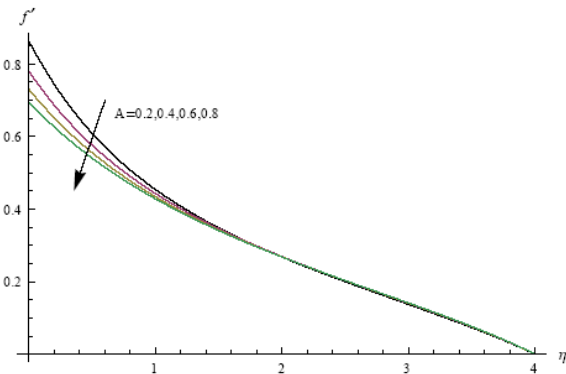


Fig.9a Variation of  $f'(\eta)$  with  $A$   
 $Sr=0.5, Ec=0.01, m=0.5, S=0.2, A1=0.1, \tau=0.1, B1=0.1$

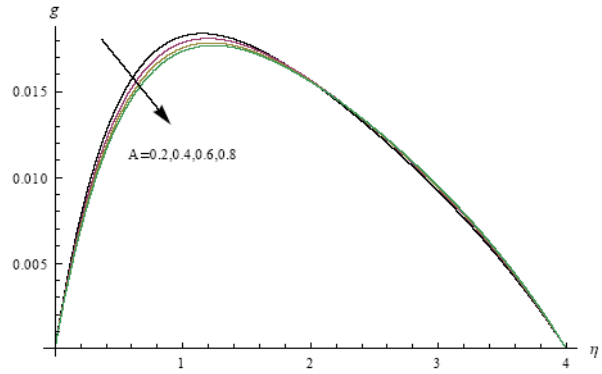


Fig.9b Variation of  $g(\eta)$  with  $\tau$   
 $Sr=0.5, Ec=0.01, m=0.5, S=0.2, A1=0.1, \tau=0.1, B1=0.1$

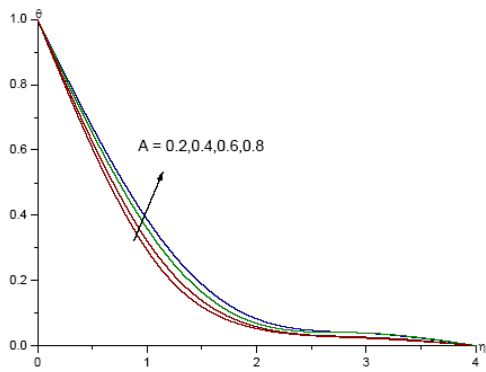


Fig.9c Variation of  $\theta(\eta)$  with  $\tau$   
 $Sr=0.5, Ec=0.01, m=0.5, S=0.2, A1=0.1, \tau=0.1, B1=0.1$

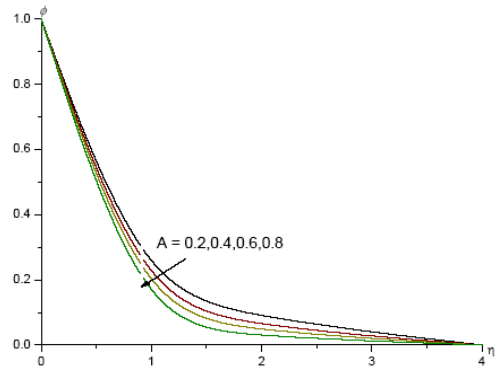


Fig.9d Variation of  $\phi(\eta)$  with  $\tau$   
 $Sr=0.5, Ec=0.01, m=0.5, S=0.2, A1=0.1, \tau=0.1, B1=0.1$

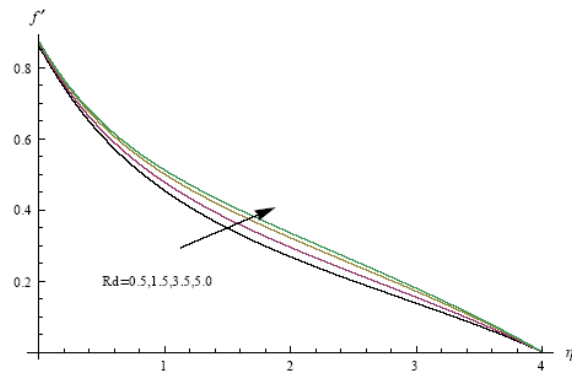


Fig.10a Variation of  $f'(\eta)$  with  $Rd$   
 $m=0.5, Sr=0.5, A1=0.1, B1=0.1, S=0.2, A=0.2, \tau=0.1$

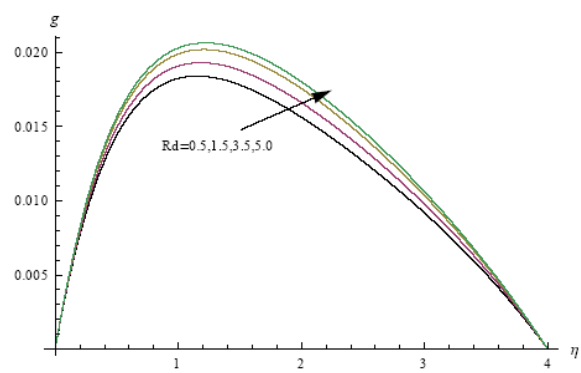


Fig.10b Variation of  $g(\eta)$  with  $Rd$   
 $m=0.5, Sr=0.5, A1=0.1, B1=0.1, S=0.2, A=0.2, \tau=0.1$

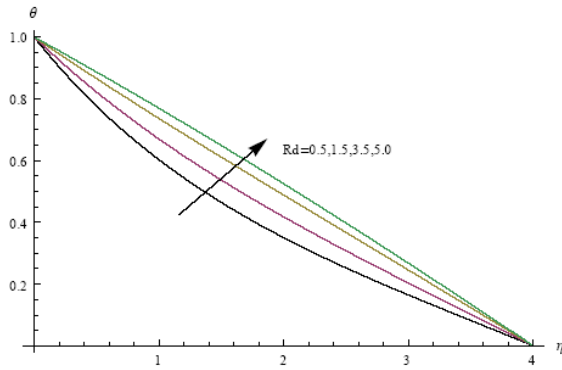


Fig.10c Variation of  $\theta(\eta)$  with Rd  
 $m=0.5, Sr=0.5, A1=0.1, B1=0.1, S=0.2, A=0.2, \tau=0.1$

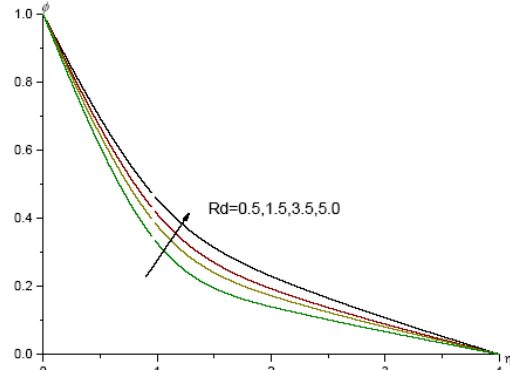


Fig.10d Variation of  $\phi(\eta)$  with Rd  
 $m=0.5, Sr=0.5, A1=0.1, B1=0.1, S=0.2, A=0.2, \tau=0.1$

**Table-1:** Skin friction ( $\tau_x$ ), Nusselt Number (Nu) at  $\eta = 0$

Parameter		$\tau_x(0)$	$\tau_z(0)$	Nu(0)	Sh(0)
<b>m</b>	<b>0.5</b>	-0.673	0.0471	0.51352	0.87656
	<b>1.0</b>	-0.6614	0.05745	0.51472	0.87637
	<b>1.5</b>	-0.636	0.05725	0.51738	0.87595
	<b>2.0</b>	-0.5652	0.0473	0.49696	0.83909
<b>Ec</b>	<b>0.01</b>	-0.673	0.0471	0.51352	0.87656
	<b>0.03</b>	-0.6728	0.0471	0.5121	0.87646
	<b>0.05</b>	-0.6727	0.04711	0.51106	0.87638
	<b>0.07</b>	-0.6728	0.0471	0.51146	0.87641
<b>A1</b>	<b>0.1</b>	-0.673	0.0471	0.51352	0.87656
	<b>0.3</b>	-0.6678	0.04738	0.48474	0.8745
	<b>-0.1</b>	-0.6778	0.04683	0.54048	0.87848
	<b>-0.3</b>	-0.63	0.05023	0.5479	0.84411
<b>B1</b>	<b>0.1</b>	-0.673	0.0471	0.51352	0.87656
	<b>0.3</b>	-0.6662	0.04747	0.47656	0.87391
	<b>-0.1</b>	-0.6791	0.04676	0.54711	0.87895
	<b>-0.3</b>	-0.6323	0.0501	0.55926	0.84492
<b>Sr</b>	<b>0.5</b>	-0.673	0.0471	0.51352	0.87656
	<b>1.0</b>	-0.6727	0.04711	0.51312	0.86622
	<b>1.5</b>	-0.672	0.04715	0.51191	0.83535
	<b>2.0</b>	-0.6175	0.05095	0.48876	0.78477
<b>S</b>	<b>0.2</b>	-0.4251	0.06536	0.40831	0.7133
	<b>0.4</b>	-0.4934	0.06016	0.43626	0.75755
	<b>0.6</b>	-0.558	0.05531	0.46321	0.79967
	<b>0.8</b>	-0.6191	0.05086	0.49104	0.84002
<b>tau</b>	<b>0.1</b>	-0.673	0.0471	0.51352	0.87656
	<b>0.2</b>	-0.6742	0.04703	0.51541	0.94482
	<b>0.3</b>	-0.6753	0.04698	0.51711	1.00927
	<b>0.5</b>	-0.6227	0.05066	0.49645	1.02977
<b>A</b>	<b>0.2</b>	-0.673	0.0471	0.51352	0.87656
	<b>0.4</b>	-0.5206	0.04448	0.50534	0.87848
	<b>0.6</b>	-0.4326	0.0429	0.50043	0.87963
	<b>0.8</b>	-0.3421	0.04591	0.47537	0.84371
<b>Rd</b>	<b>0.5</b>	-0.673	0.0471	0.51352	0.87656
	<b>1.5</b>	-0.6509	0.04828	0.38893	0.86771
	<b>3.5</b>	-0.6296	0.04944	0.27596	0.85965
	<b>5.0</b>	-0.6155	0.0502	0.20499	0.85458

## 6. CONCLUSIONS

The non-linear equations governing the flow heat and mass transfer have been solved by using Runge-Kutta Shooting technique. From the graphical representations and tabular values we find that

- Higher the thermo-diffusion effect larger the velocities, and concentration and smaller the temperature in the flow region. The rate of heat and mass transfer reduces with Sr.
- Higher the dissipation larger the velocities, temperature and smaller the concentration. The Nusselt number enhances and the Sherwood number reduces with increase in Ec.

- An increase in Thermophoresis parameter ( $\tau$ ) reduces velocities, temperature and concentration. The Nusselt and Sherwood number on the wall enhance with increase in  $\tau$ .
- An increase in slip parameter (A) reduces the velocities, concentration and enhances the temperature. The Nusselt number reduces and the Sherwood number enhances with increase in A.
- Higher the radiative heat flux larger the velocities, temperature and concentration in the flow region. The Nusselt and Sherwood number depreciates on the wall with increase in Rd.

## 7. REFERENCES

1. Abo-Eldahab E.M., and El-Gendy M.S.: Heat current and ohmic heating effect on mixed convection boundary layer flow of amicro-polar fluid from a rotating cone with power-law variation in surface temperature, *Int. Commun.HeatMass Transfer*, 31,751-762, 2004.
2. Ali, M.E.: Heat transfer characteristics of a continuous stretching surface, *Heat mass transfer*, 29, 227-234, (1994).
3. Aliveli B, Sreevani M : Convective heat and mass transfer flow of viscous fluid with variable viscosity in the presence of thermophoresis particle deposition, *International Journal for Research & Development in Technology*, Vol.8, Issue 5 (2017), Issn 2349-3585, web.www.ijrdt.org.
4. Anwar Beg O, Takhar H.S., Bhargava R, Rawat S, and Prasad V.R.: Numerical study of heat transfer of a third grade viscoelastic fluid in non-Darcian porous media with thermo physical effects, *Phys. Scr*, 77, 1-11 (2009).
5. Bhargava R, Sharma R and Beg O.A : Oscillatory chemically-reacting MHD free convection heat and mass transfer in a porous medium with Soret and Dufour effects, finite element modelling, *Int.J. Appl.Math.Mech*, 5 (6), 15-3 (2009).
6. Chamkha A.J, and Rashad A.M.: Unsteady heat and mass transfer by MHD mixed convection flow from a rotating vertical cone with chemical reaction and Soret and Dufour effects, *The Canadian Journal of Chemical Engineering*, DOI 10.1002/cjce 21894, (2014).
7. Crane, L.J., *Z. Angew. Math. Phys*, 21, pp. 645–647 (1970).
8. Damseh R.A., Tahat M.S, and Benim A.C, Non-similar solutions of magnetohydrodynamic and thermophoresis particle deposition on mixed convection problem in porous media along a vertical surface with variable wall temperature, *Progress in Computational Fluid Dynamics* 9(1), 58-65, (2009).
9. Dinesh K.K., and Jayaraj S, Augmentation of thermophoretic deposition in natural convection flow through a parallel plate channel with heat sources, *Int. Communications Heat and Mass Transfer* 36, 931-935 (2009).
10. Dulal Pal, and Mondal. H, MHD non-Darcian mixed convection heat and mass transfer over a non-linear stretching sheet with Soret and Dufour effects and chemical reaction, *International communications in heat and mass transfer*, 463-467 (2011).
11. Dulal pal, Combined effects of non-uniform heat source/sink and thermal radiation on heat transfer over an unsteady stretching permeable surface, *Commun Nonlinear Sci Numer Simulat*, 16, 1890-1904, (2011).
12. Duwairi H.M., Damseh R.A., Effect of thermophoresis particle deposition on mixed convection from vertical surfaces embedded in saturated porous medium, *Int. J.Numerical Methods Heat Fluid Flow*, 18(2), 202-216 (2008).
13. Elbashbeshy EMA and Bazid MAA: Heat transfer over an unsteady stretching surface, *Heat Mass Transfer*, 41, 1-4, (2004).
14. Eshetu Haile, and Shankar B : Heat and Mass Transfer in a Boundary Layer of Unsteady Viscous Nano fluid along a Vertical Stretching Sheet, *Journal of Computational Engineering*, DOI/10.1155/2014/345153, (2014).
15. Grosan T, Pop R, and Pop I, Thermophoretic deposition of particles in fully developed mixed convection flow in parallel plate vertical channel, *Heat Mass Transfer* 45, 503-509, (2009).
16. Grubka L.G. and Bobba K.M., Heat transfer characteristics of a continuous stretching surface with variable temperature, *J.Heat Transfer – Trans. ASME*.107, P.248-250 (1985)
17. Gupta, P.S., Gopta, A.S: Heat and Mass Transfer on a stretching sheet with suction or blowing, *can.J.Chem.Eng*, 55, pp. 744-746 (1977).
18. Hayat T, Javed T, Sajid M: Analytic solution for MHD rotating flow of a second grade fluid over a shrinking surface. *Phys. Lett. A* 372: 3264–3273(2008).
19. Ishak A: Unsteady MHD flow and heat transfer over a stretching plate, *J. Applied Sci*, 10(18), 2127-2131 (2010).
20. Ishak A, Nazar R, and Pop I, Heat transfer over an unsteady stretching permeable surface with prescribed wall temperature, *Nonlinear Anal: Real World Appl*, 10, 2909-13, (2009).
21. Ishak, A, Nazar R, and Pop I.: Boundary layer flow and heat transfer over an unsteady stretching vertical surface, *Meccanica*, 44, 369-375 (2009).
22. Liu Z, Chen Z, and Shi M, Thermophoresis of particles in aqueous solution in micro channel, *Applied Thermal Engineering*, 29, (5-6), 1020-1025, (2009).
23. Mahdy A, Hady f.M., Effect of thermophoretic particle deposition in non-Newtonian free convection flow over a vertical plate with magnetic field effect, *Journal of Non-Newtonian fluid Mechanics*, 161 (1-3), 37-41 (2009).

24. Makinde, O.D, On MHD Mixed Convection with Soret and Dufour Effects Past a Vertical Plate Embedded in a Porous Medium, *Latin American Applied Research* 42, 63-68 (2011).
25. Mansour M.A., and El-Shaer N.A., Radiative effects on magnetohydrodynamic natural convection flows saturated in porous media, *J. Magn.Mater*, 237,327-341, (2001).
26. Molla Md. M, Saha S.C., and Hossain Md.A: Radiation effect on free convection laminar flow along a vertical flat plate with stream wise sinusoidal surface temperature, *Math. Comput. Modeling*, 53, 1310-1319, (2011).
27. Mustafa M: Cattaneo-Christov heat flux model for rotating flow and heat transfer of upper-convected Maxwell fluid. *AIP Advances* 5: doi: 10.1063/1.4917306 (2015)
28. Nazar R, Amin N, Pop I: Unsteady boundary layer flow due to a stretching surface in a rotating fluid. *Mech. Res. Commun.* 31: 121–128(2004).
29. Pal D, Heat and mass transfer in stagnation-point flow towards a stretching surface in the presence of buoyancy force and thermal radiation, *Meccanica*, 44,145-158, (2005).
30. Pal. D, and Mandal H, The influence of thermal radiation on hydromagnetic Darcy-Forchheimer mixed convection flow past a stretching sheet embedded in a porous medium, *Meccanica*, doi:10.1007/s 11012-010-9334-8, (2010)
31. Plumb O.A., Huenfield J.S., and Eschbach E.J., The effect of cross flow and radiation on natural convection from vertical heated surfaces in saturated porous media, in : *AIAA 16th Thermophysics conference*, June 23-25, Palo Alto, California, USA, (1981).
32. Postelnicu A, Effects of thermophoresis particle deposition in free convection boundary layer from a horizontal flat plate embedded in a porous medium, *Int. J. Heat Mass Transfer* 50 (15-16), 2981-2985 (2007).
33. Rajeswari V, Nath G (1992) Unsteady flow over a stretching surface in a rotating fluid. *Int. J. Eng. Sci.* 30: 747–756.
34. Rana P, and Bhargava R, Flow and heat transfer of a Nano fluid over a nonlinearly stretching sheet: a numerical study, *Comm. Nonlinear Sci. Numer. Similat*, 17, 212-226, 2012.
35. Rashidi MM, Abelman S, Mehr NF : Entropy generation in steady MHD flow due to a rotating porous disk in a nanofluids. *Int J. Heat Mass Transf*, 62: 515–525 (2013).
36. Reddy J.N.: *An Introduction to the Finite Element Method*, McGraw-Hill Book Co., New York, (1985).
37. Reddy P.S. and Rao V.P. : Thermo-Diffusion and Diffusion – Thermo Effects on Convective Heat and Mass Transfer through a Porous Medium in a Circular Cylindrical Annulus with Quadratic Density Temperature Variation – Finite Element Study, *Journal of Applied Fluid Mechanics*, 5(4), 139-144, (2012).
38. Sheikholeslami M, Hatami M, Ganji DD: Nanofluid flow and heat transfer in a rotating system in the presence of a magnetic field. *J. Mol. Liq.* 190: 112–120 (2014).
39. Sikiadis B.C., Boundary layer behavior on continuous solid surfaces, *ICChE J.7*, 26-28, (1961)
40. Sivagopal R, Siva Prasad R : Soret and Dufour effects on MHD heat and mass transfer flow of a micropolar fluid over stretching sheet through porous medium with thermo-phoresis, *International Journal of Advanced Scientific and Technical Research* ,Issue 6 volume 5, September-October 2016 web: www.rpublication.com, ISSN:2249-9954, Impact Factor 3.6.
41. Sreenivasa Reddy B: Soret and Dufour effect on convective heat and mass transfer flow of a micro polar fluid in presence of thermoporosus deposition particle, *National Conference on Emerging Research Trends in Pure and Applied Mathematics*, S.P. Mahila University, Tirupati, 2017
42. Sreenivasa Reddy B, Madhusudhana K and Sreedhar Babu M : The effect of thermoporosus on convective heat and mass transfer flow past stretching sheet with Soret and Dufour effect, *International Research Journal of Mathematics, Engineering and I.T.*, Vol.3(6), (2015).
43. Talbot L, Cheng R.K., Schefer R.W., and et al, Thermophoresis of particles in a heated boundary layer. *J. FluidMech*, 101(4), 737-758, (1980)
44. Tsai R, and Huang J.S, Combined effects of thermophoresis and electrophoresis on particle deposition onto a vertical flat plate from mixed convection flow through a porousmedium. *Chemical Eng., J.* 157, 52-59, (2010).
45. Tsai R, Huang K.H, and Huang J.S.: Flow and heat transfer over an unsteady stretching surface with non-uniform heat source, *Int. Commun. Heat Mass Transfer*, 35, 1340-1343, (2008).
46. Tsou, F.K., Sparrow, E.M. and Goldstein, R.J: Flow and heat transfer in the boundary layer on a continuous moving surface, *Int. J. Heat Mass Transfer* 10, pp. 219–235 (1967).
47. Vajravelu K, and Rollis D : Heat transfer in electrically conducting fluid over a stretching surface, *Internat. J. Non-linear mech*, 27(2), 265-277, (1992)
48. Vajravelu, K, Flow and heat transfer in a saturated over a stretching surface, *ZAMM. V.* 74, pp. 605-614, (1994).
49. Wang CY: Liquid film on an unsteady stretching surface, *Q. Appl. Math*, 48, 6601-10, (1990).
50. Wang CY: Stretching a surface in a rotating fluid, *ZAMP* 39; 177-185, (1988).
51. Zaimi K, Ishak A, Pop I: Stretching surface in rotating viscoelastic fluid. *Appl. Math. Mech.* 34: 945–952 (2013).

**Source of support: Nil, Conflict of interest: None Declared.**

**[Copy right © 2019. This is an Open Access article distributed under the terms of the International Journal of Mathematical Archive (IJMA), which permits unrestricted use, distribution, and reproduction in any medium, provided the original work is properly cited.]**